A Fundamental Equation of State for the (R134a + Triethylene Glycol Dimethyl Ether) Mixture

Paolo Marchi, and Giancarlo Scalabrin
Dipartimento di Fisica Tecnica, Università di Padova, via Venezia 1, I-35131 Padova, Italy

E. Christian Ihmels
Laboratory for Thermophysical Properties LTP GmbH, Marie-Curie-Straße 10, D-26129 Oldenburg, Germany

Dominique Richon
Centre Energétique et Procédés, Ecole Nationale Supérieure des Mines de Paris CEP/TEP, CNRS FRE 2861, 35 rue Saint Honoré, F-77305 Fontainebleau, France

DOI 10.1002/aic.11166
Published online April 3, 2007 in Wiley InterScience (www.interscience.wiley.com).

The thermodynamic properties of the mixture of 1,1,1,2-tetrafluoroethane (R134a) and triethylene glycol dimethyl ether (TriEGDME) have been modeled with equations of state in an extended corresponding states format. A recent equation of state for pure R134a was assumed as the reference while the scale factors have been obtained in neural network form by regression of experimental data for the mixture. The modeling was focused on the liquid phase, considering the possible application of such a mixture in a refrigeration plant; since the vapor pressure of pure TriEGDME is negligible over the considered temperature range, the vapor phase of the mixture at vapor-liquid equilibrium condition is almost pure R134a. Two fundamental equations are proposed herein. The first one, developed from a limited amount of experimental data is valid for R134a mole fractions greater than 0.94. The second equation was obtained from a wider data base; it has a larger number of free parameters to regress and covers the R134a mole fractions greater than 0.59. © 2007 American Institute of Chemical Engineers *AIChE J,* 53: 1349–1361, 2007
Keywords: extended corresponding states, neural networks, R134a, refrigerant + lubricant mixtures, thermodynamic properties, TriEGDME

Introduction

The environmental problems connected with the use of chlorofluorocarbon (CFC) refrigerants, in particular the depletion of the stratospheric layer of ozone, have imposed the phase-out of such substances and their replacement with less harmful fluids. Consequently, the study of alternative refrigerants and of their properties has become a fundamental task for scientific and technical research.

Correspondence concerning this article should be addressed to G. Scalabrin at gscala@unipd.it.

Nowadays, the fluids mainly used in the refrigeration and air-conditioning plants are hydrofluorocarbons (HFC) that show better environmental behavior, thanks to the absence of chlorine atoms in their molecules. Among the substances of this family, 1,1,1,2-tetrafluoroethane (R134a) is widely used, because of its favorable thermodynamic performances in compression cycles and its compatibility with the existing refrigeration plants designed for CFC refrigerants.

The identification of a suitable alternative refrigerant does not completely solve the technical problem: in fact, in the compression plants, the working fluid is not a pure refrigerant (or a mixture of refrigerants), but a certain amount of lubricant, compatible and soluble with the refrigerant, must be added. Because the mineral oils that were used with CFCs for years show low solubility in HFC refrigerants, it is necessary to propose alternative lubricants.

The problems posed by the selection of the lubricant have been widely studied in recent years; a partial review is given by Marsh and Kandil.[1] Guidance for the choice of the most efficient lubricant for specific technical applications, as for instance the design of a refrigeration plant, requires the knowledge of the thermophysical properties of the refrigerant + lubricant mixtures.

Polyalkylene glycols (PAGs) were proposed as suitable lubricants in combination with R134a. Several researchers have focused their attention on such mixtures: measurements of solubility data,[2–7] of density data,[8–11] and of viscosity data[8,12–14] were produced.

A technical lubricant is usually a mixture of several components sharing the same chemical structure, e.g. PAGs, in which few of them are prevailing in composition; some additives are furthermore added to this mixture. The final product, marketed with a producer's trademark, is a proprietary blend.

Since it is very difficult to characterize such a complex mixture with sufficient precision from the chemical and thermophysical points of view, it is preferable to start the present study from the thermodynamic behavior of a simple refrigerant + lubricant mixture, then avoiding technical lubricants. Therefore, at this step of the study, it is better to assume the lubricant to be an equivalent pure compound. For these purposes, we chose triethylene glycol dimethyl ether (TriEGDME).

Some works aiming at modeling the thermodynamic properties of the refrigerant + lubricant mixtures were published in the literature,[15–22] but they mainly addressed the representation of the vapor–liquid equilibrium. These works are based either on the modified Flory–Huggins model, on cubic equations of state (including or not a modified UNIFAC model), or on perturbed-hard-sphere-chain equations of state. Several of them have quite good performances in representing bubble pressures at equilibrium conditions, but their capability in describing the whole thermodynamic behavior, as for instance density and calorimetric quantities in the compressed liquid region, is not known. Considering that the aforementioned types of equations are in general not suitable to represent both thermal and caloric properties, it is expected that the cited models also lack in accuracy when describing the thermodynamic properties of a refrigerant + lubricant mixture in the liquid region.

The goal of the present work is the development of a dedicated equation of state (DEoS) for the binary mixture of R134a and TriEGDME. Since the lubricant content in the working fluid of a refrigeration plant is usually less than 10% in mass fraction, this is also the main range of interest. The format chosen for the DEoS is based on the extended corresponding states (ECS) model, into which a neural network (NN) was integrated to increase its flexibility. This technique, in the following referred to as ECS-NN, can be applied to both pure fluids and mixtures, as it was widely described in previous works.[23–25]

The obtained DEoS is a *fundamental* equation of state, because it is expressed in terms of Helmholtz energy, from which all of the thermodynamic properties can be directly calculated through simple mathematical derivations. The regression of the equation parameters is done using the available experimental data, part of which were specifically produced for the present modeling purpose.[7,11]

The ECS-NN Modeling Technique

The ECS-NN modeling technique was presented in detail in previous articles[23–25] and only a brief summary is given here for reader's convenience.

The corresponding states principle, whose derivation from statistical mechanics is given by Reed and Gubbins[26] and Rowlinson and Swinton,[27] states the equality of the reduced residual Helmholtz energy a^{R}:

$$a^{\mathrm{R}}(T,\rho) = \frac{A(T,\rho) - A^{\mathrm{ig}}(T,\rho)}{RT} \tag{1}$$

for two *conformal* pure fluids when evaluated at the same reduced conditions:

$$a_j^{\mathrm{R}}(T_{\mathrm{r}},\rho_{\mathrm{r}}) = a_0^{\mathrm{R}}(T_{\mathrm{r}},\rho_{\mathrm{r}}) \tag{2}$$

where the subscript j indicates the fluid of interest and 0 denotes a reference fluid whose thermodynamic properties are accurately known from a DEoS. In Eq. 1, the superscript ig refers to an ideal-gas condition. Since the equations in terms of Helmholtz energy are fundamental equations of state, all of the thermodynamic properties of the fluid of interest can be calculated through derivations of Eq. 2 with respect to temperature and density. The fulfillment of the *conformality* condition requires that the two fluids obey the same reduced intermolecular force law; such a condition is verified for a limited number of fluids with spherically-symmetric molecules, as for instance the noble gases.

The ECS method[28–31] aims at extending a similar model structure to other fluids, bypassing the conformality requirement. The basic equation of the model ECS is similar to Eq. 2:

$$a_j^{\mathrm{R}}(T_j,\rho_j) = a_0^{\mathrm{R}}(T_0,\rho_0) \tag{3}$$

but here the temperatures and the densities of the fluids are related through two functions f_j and h_j, called *scale factors*, that depend on the thermodynamic variables of the fluid of interest:

$$T_0 = \frac{T_j}{f_j(T_j,\rho_j)} \tag{4}$$

$$\rho_0 = \rho_j h_j(T_j,\rho_j) \tag{5}$$

If the system of interest is a mixture, denoted by subscript m, Eq. 3 is transformed into

$$a_{\mathrm{m}}^{\mathrm{R}}(T_{\mathrm{m}},\rho_{\mathrm{m}},\bar{x}) = a_0^{\mathrm{R}}(T_0,\rho_0) \tag{6}$$

where $\bar{x}$ is the array of the mole fractions. In this case, the scale factors f_{m} and h_{m} depend also on mole fraction:

$$T_0 = \frac{T_{\mathrm{m}}}{f_{\mathrm{m}}(T_{\mathrm{m}},\rho_{\mathrm{m}},\bar{x})} \tag{7}$$

$$\rho_0 = \rho_{\mathrm{m}} h_{\mathrm{m}}(T_{\mathrm{m}},\rho_{\mathrm{m}},\bar{x}) \tag{8}$$

The availability of the equations for the scale factors and of an accurate DEoS for the reference fluid allows the calculation of all the thermodynamic properties of the target sys-

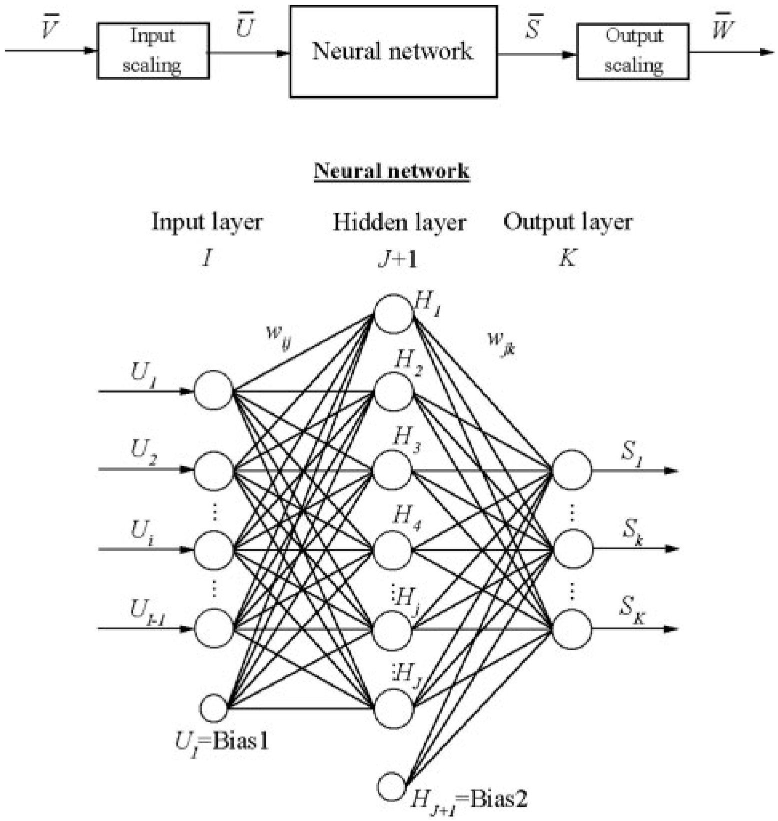

Figure 1. General topology of a three-layer feedforward neural network.

tem. A summary of the main mathematical relations required for this purpose is given in the Appendix.

Several methods are published in the literature to obtain and represent the scale factors.[23–25,28–37] The technique adopted here, developed by Scalabrin et al.,[24] assumes a multilayer feedforward neural network (MLFN) as an analytical form of the scale factor functions; the coefficients of the neural network are regressed from experimental data of thermodynamic properties for the system of interest.

The general architecture of a MLFN is illustrated in Figure 1: it is constituted by a certain number of units, called *neurons*, organized in three layers called the *input*, *hidden*, and *output* layers, respectively. The neurons of the input layer are indicated as elements of an array $\overline{U}$ of dimension I. Their number coincides with the number of independent variables of the equation plus one. The last neuron, labeled Bias1, has a constant value:

$$U_I = \text{Bias 1} \tag{9}$$

The number of neurons in the output layer equals the output quantities, which are elements of an array $\overline{S}$ of dimension K.

The hidden layer performs the transformation of the signals from the input layer to the output layer, and it can contain an arbitrary number of neurons. These are elements of an array $\overline{H}$ of dimension $J + 1$. Also in the hidden layer, there is a bias neuron with a constant value, Bias2:

$$H_{J+1} = \text{Bias2} \tag{10}$$

The physical input variables V_i (in the present case temperature, density, and mole fraction) undergo a linear transformation to normalize them in the arbitrarily chosen range [$A_{\min}$, $A_{\max}$] set at $A_{\min} = 0.05$ and $A_{\max} = 0.95$:

$$U_i = u_i\left(V_i - V_{i,\min}\right) + A_{\min} \qquad \text{for } 1 \le i \le I-1 \tag{11}$$

where

$$u_i = \frac{A_{\max} - A_{\min}}{V_{i,\max} - V_{i,\min}} \tag{12}$$

and $V_{i,\min}$ and $V_{i,\max}$ represent the selected extremes of the range of the variable V_i.

An arctangent function normalized in the range [0, 1] is assumed as the transfer function g:

$$g(z) = \frac{1}{\pi}\arctan(0.1\, z) + 0.5 \tag{13}$$

The transfer function calculates the signal output of a neuron from its inputs for both the hidden and the output layer neurons; respectively it is:

Table 1. Molar Masses and Critical Parameters for R134a and TriEGDME

	R134a	TriEGDME
CAS-RN	811-97-2	112-49-2
M (kg mol^{-1})	0.10203	0.17823
T_c (K)	374.083	636.371*
P_c (MPa)	4.048	2.3703*
ρ_c (mol l^{-1})	4.9887	1.800*

*Calculated from Joback group contribution method.[39]

Table 2. Coefficients of the ECS-NN Equation of State (DEoS-1) Valid in the Narrower Range (see Table 4)

$I = 4$		$J = 2$	$K = 2$			Bias1		1.00	Bias2		1.00
$V_{1,\mathrm{min}} = T_{\mathrm{m,min}}$		270 K	$V_{1,\mathrm{max}} = T_{\mathrm{m,max}}$		340 K	$W_{1,\mathrm{min}} = \tilde{f}_{\mathrm{m,min}}$		1.00	$W_{1,\mathrm{max}} = \tilde{f}_{\mathrm{m,max}}$		1.50
$V_{2,\mathrm{min}} = \rho_{\mathrm{m,min}}$		8 mol l^{-1}	$V_{2,\mathrm{max}} = \rho_{\mathrm{m,max}}$		14 mol l^{-1}	$W_{2,\mathrm{min}} = \tilde{h}_{\mathrm{m,min}}$		1.80	$W_{2,\mathrm{max}} = \tilde{h}_{\mathrm{m,max}}$		2.20
$V_{3,\mathrm{min}} = x_{\mathrm{min}}$		0.93	$V_{3,\mathrm{max}} = x_{\mathrm{max}}$		1.00	A_{min}		0.05	A_{max}		0.95
i	j	w_{ij}	i	j	w_{ij}	j	k	w_{jk}	j	k	w_{jk}
1	1	−40.8585	1	2	−3.87945	1	1	101.023	2	2	10.7578
2	1	−74.4033	2	2	26.6931	2	1	40.8661	3	2	13.4079
3	1	31.5027	3	2	−3.09506	3	1	−11.1543			
4	1	−12.6105	4	2	−25.5864	1	2	29.9422			

Table 3. Coefficients of the ECS-NN Equation of State (DEoS-2) Valid in the Wider Range (see Table 4)

$I = 4$		$J = 5$	$K = 2$			Bias1		1.00	Bias2		1.00
$V_{1,\mathrm{min}} = T_{\mathrm{m,min}}$		270 K	$V_{1,\mathrm{max}} = T_{\mathrm{m,max}}$		340 K	$W_{1,\mathrm{min}} = \tilde{f}_{\mathrm{m,min}}$		1.00	$W_{1,\mathrm{max}} = \tilde{f}_{\mathrm{m,max}}$		1.50
$V_{2,\mathrm{min}} = \rho_{\mathrm{m,min}}$		7.5 mol l^{-1}	$V_{2,\mathrm{max}} = \rho_{\mathrm{m,max}}$		14 mol l^{-1}	$W_{2,\mathrm{min}} = \tilde{h}_{\mathrm{m,min}}$		1.80	$W_{2,\mathrm{max}} = \tilde{h}_{\mathrm{m,max}}$		2.20
$V_{3,\mathrm{min}} = x_{\mathrm{min}}$		0.55	$V_{3,\mathrm{max}} = x_{\mathrm{max}}$		1.00	A_{min}		0.05	A_{max}		0.95
i	j	w_{ij}	i	j	w_{ij}	i	j	w_{ij}	j	k	w_{jk}
1	1	−7.32136	2	3	82.4862	3	5	−44.8330	6	1	−66.7043
2	1	42.2617	3	3	−40.8621	4	5	48.9830	1	2	−21.6182
3	1	−9.58943	4	3	−17.2587				2	2	3.13025
4	1	−14.5974	1	4	31.3384	j	k	w_{jk}	3	2	10.3838
1	2	−34.2833	2	4	45.9064	1	1	0.759467	4	2	22.4568
2	2	−35.3536	3	4	13.3882	2	1	3.57306	5	2	35.0301
3	2	62.4382	4	4	2.80395	3	1	−0.759281	6	2	−55.6304
4	2	36.4986	1	5	−4.30323	4	1	111.609			
1	3	−8.61226	2	5	20.6424	5	1	−51.7583			

Table 4. Validity Limits of the Proposed ECS-NN Equations of State

	DEoS-1	DEoS-2
T (K)	280–325	280–335
P (MPa)	≤ 6	≤ 60
x	0.94–1.00	0.59–1.00

$$H_j = g\left(\sum_{i=1}^{I} w_{ij} U_i\right) \qquad \text{for } 1 \leq j \leq J \tag{14}$$

$$S_k = g\left(\sum_{j=1}^{J+1} w_{jk} H_j\right) \qquad \text{for } 1 \leq k \leq K \tag{15}$$

The symbols w_{ij} and w_{jk} indicate the *weighting factors* that are the free parameters of the model, which must be determined in the regression process.

The output values S_k of the output layer neurons are denormalized to real output variables W_k, which are in this case the scale factors f_m and h_m, through the following linear transformation:

$$W_k = \frac{S_k - A_{\min}}{s_k} + W_{k,\min} \qquad \text{for } 1 \leq k \leq K \tag{16}$$

where

$$s_k = \frac{A_{\max} - A_{\min}}{W_{k,\max} - W_{k,\min}} \tag{17}$$

$W_{k,\min}$ and $W_{k,\max}$ are the chosen limits of the range of the dependent variable W_k.

After the regression of the weighting factors, the neural network can be used to calculate the values of the scaling factors as functions of temperature, density, and mole fraction of the system of interest.

The Equations of State for the (R134a + TriEGDME) System

The critical parameters for R134a were taken from the recent work of Astina and Sato,[38] whereas for TriEGDME the values were calculated by the group contribution method of Joback.[39] These parameters, together with the molar masses of the two pure components, are given in Table 1.

The reduced Helmholtz energy a_m of the mixture can be expressed as the summation of two terms: the ideal-gas part a_m^{ig} and the residual part a_m^R:

$$\begin{aligned} a_m(T_m, \rho_m, x) &= \frac{A_m(T_m, \rho_m, x)}{RT_m} \\ &= a_m^{ig}(T_m, \rho_m, x) + a_m^R(T_m, \rho_m, x) \end{aligned} \tag{18}$$

where x is the mole fraction of R134a and the subscript m indicates that the properties are referred to the mixture. The value $R = 8.314472$ J mol^{-1}K^{-1}, reported by Mohr and Taylor,[40] was assumed for the universal gas-constant.

As explained hereafter, in this work, two equations with different validity ranges have been developed for the system. Both the equations are valid only for the liquid region; in fact, at the considered conditions, the vapor phase in equilibrium with the liquid one is essentially composed of pure R134a, as the vapor pressure of pure TriEGDME is very low and negligible. For pure R134a, a multiparameter DEoS in terms of Helmholtz energy was developed by Astina and Sato.[38]

The relations for the calculation of the thermodynamic properties are given in the Appendix. For the vapor–liquid equilibrium (VLE), the isofugacity condition for R134a has to be solved for the bubble pressure (P_{bubble}):

$$f_1^v(T_m, P_{\text{bubble}}) = \hat{f}_1^l(T_m, P_{\text{bubble}}, x) \tag{19}$$

In Eq. 19, f_1^v is the fugacity of pure R134a in the vapor phase at the same (T, P) conditions of the mixture and it is calculated from the DEoS of Astina and Sato;[38] $\hat{f}_1^l$ is the partial molar fugacity of the same component in the liquid phase and it is obtained from the proposed mixture DEoS.

The two contributions involved in Eq. 18 are separately studied in the following parts.

Ideal-Gas Contribution

The ideal-gas contribution (a_m^{ig}) of the mixture is analytically obtained from the linear combination of the ideal-gas contributions (a_i^{ig}) of the pure components, plus the ideal change of mixing:

$$\begin{aligned} a_m^{ig}(T_m, \rho_m, x) = x a_1^{ig}(T_m, \rho_m) + (1-x) a_2^{ig}(T_m, \rho_m) \\ + [x \ln x + (1-x) \ln(1-x)] \end{aligned} \tag{20}$$

The ideal-gas contribution for each pure fluid is developed from an equation for its ideal-gas isobaric heat capacity $C_{p,i}^{ig}$:

$$\begin{aligned} a_i^{ig}(T, \rho) = \frac{H_{i,o}^{ig}}{RT} - \frac{S_{i,o}^{ig}}{R} - 1 + \ln\left(\frac{\rho T}{\rho_o T_o}\right) \\ + \frac{1}{T}\int_{T_o}^{T} \frac{C_{p,i}^{ig}}{R} dT - \int_{T_o}^{T} \frac{C_{p,i}^{ig}}{RT} dT \end{aligned} \tag{21}$$

where the constants $H_{i,o}^{ig}$ and $S_{i,o}^{ig}$ are the selected values for enthalpy and entropy, respectively, in the ideal-gas state at chosen reference conditions (T_o, ρ_o).

The equation for the ideal-gas isobaric heat capacity for R134a was obtained from Astina and Sato.[38] Since neither

Table 5. Deviations of DEoS-1 with Respect to the Experimental Data

Property	Ref.	NPT	T Range (K)	P Range (MPa)	x Range	AAD (%)	Bias (%)	MAD (%)
Density	11	90	283.3–323.4	1.0–6.0	0.949–0.980	0.017	−0.002	0.054
Bubble pressure	7	76	282.6–322.8	0.4–1.3	0.941–1.000	0.153	−0.082	0.600

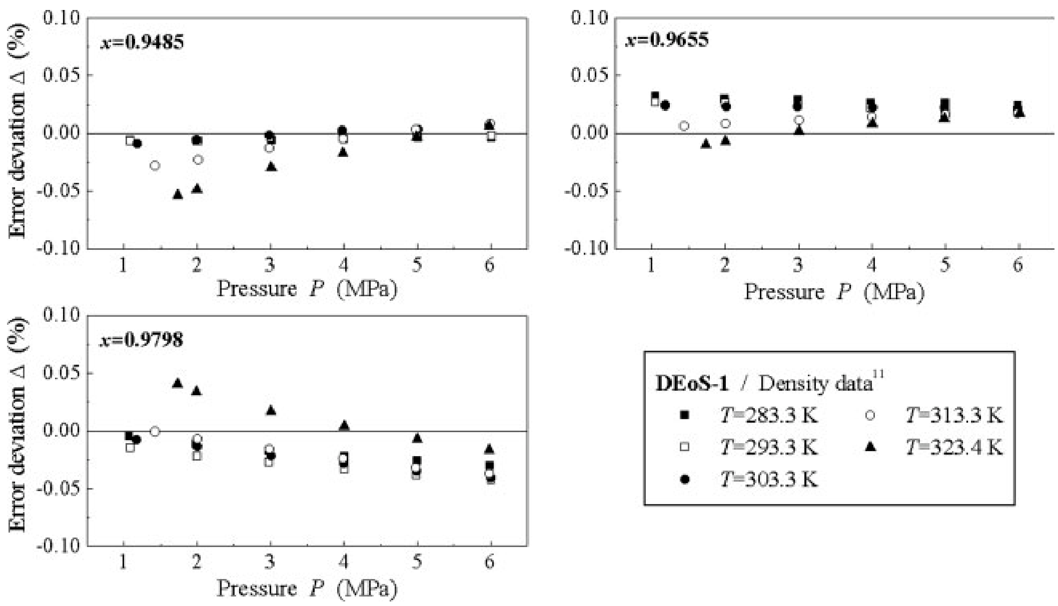

Figure 2. Deviations of the experimental density data of Marchi et al.[11] from DEoS-1.

an EoS nor suitable data are available for TriEGDME, the group contribution method of Joback[39] was used giving the equation:

$$\frac{C_{p,2}^{\mathrm{ig}}}{R} = 11.7405 + 6.14639 \times 10^{-2}\, T + 3.92087 \times 10^{-6}\, T^2 - 1.62608 \times 10^{-8}\, T^3 \qquad (22)$$

Residual Contribution

The ECS-NN format was used for modeling the residual contribution of the mixture equation. This format is particularly suitable for the representation of thermodynamics of mixtures that are very rich in one component. The assumption of such a component as the reference fluid of the ECS-NN model makes it easier to model the mixture because the mixture behavior only deviates to a limited extent from the reference fluid behavior.[24] Since R134a is the main component in the considered composition interval and a high-accuracy DEoS is available for it, this fluid was adopted as the reference fluid and its DEoS from Astina and Sato[38] was assumed as the reference equation.

A slight modification was introduced with respect to the ECS-NN model presented in a previous work.[24] Denoting with $\tilde{f}_{\mathrm{m}}$ and $\tilde{h}_{\mathrm{m}}$ the output variables W_1 and W_2 of the neural

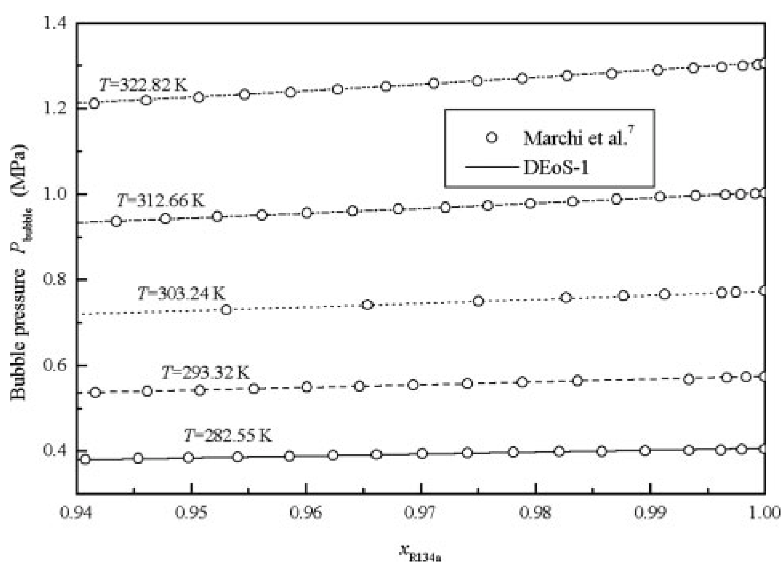

Figure 3. Bubble pressure as a function of liquid mole fraction, obtained from DEoS-1 and experimental data.

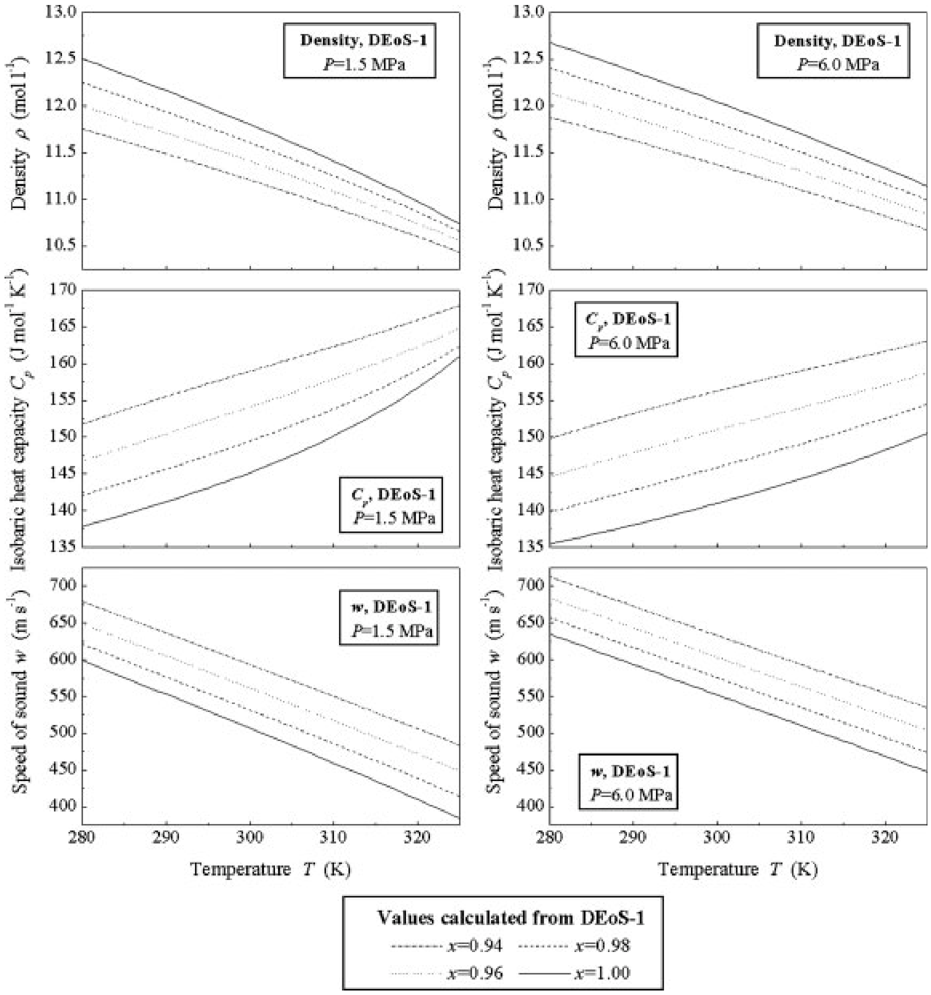

Figure 4. Values of density, isobaric heat capacity, and speed of sound at fixed mole fraction and pressure, generated from DEoS-1.

model, the scale factors to be introduced into Eqs. 7 and 8 are here obtained as:

$$f_{\mathrm{m}} = 1 + (1 - x)\widetilde{f}_{\mathrm{m}} \tag{23}$$

$$h_{\mathrm{m}} = 1 + (1 - x)\widetilde{h}_{\mathrm{m}} \tag{24}$$

Such a format is advantageous, because for $x = 1$, i.e. for pure refrigerant, both the scale factors assume a unit value and the mixture DEoS becomes equivalent to the high accuracy equation for R134a assumed as reference.

The weighting factors matrixes $\overline{w}_{ij}$ and $\overline{w}_{jk}$ of the neural network were regressed on experimental data of density and bubble pressure for the mixture, following the procedure already by Scalabrin et al.[24]

This modeling technique allows the development of an accurate fundamental DEoS for the refrigerant + lubricant mixture without the need of any detailed thermodynamic representation of the lubricant, which can be either a pure compound as in this case or a complex mixture as in the case of a technical lubricant.

Two equations were developed. The first one is valid for mole fractions of R134a greater than 0.94, that is approximately equivalent to a mass fraction greater than 0.90. For the present problem, two neurons in the hidden layer ($J = 2$) were used and the regression of the resulting 14 parameters

Table 6. Deviations of DEoS-2 with Respect to the Experimental Data

Property	Ref.	NPT	T Range (K)	P Range (MPa)	x Range	AAD (%)	Bias (%)	MAD (%)
Density	9	225	293.1–333.1	5.0–60.0	0.602–1.000	0.018	0.009	0.097
	11	90	283.3–323.4	1.0–6.0	0.949–0.980	0.027	−0.004	0.076
	Total	*315*	*283.3–333.1*	*1.0–60.0*	*0.602–1.000*	*0.021*	*0.005*	*0.097*
Bubble pressure	4	24	283.1–333.1	0.2–1.4	0.592–0.903	0.670	−0.427	1.425
	7	125	282.6–322.8	0.3–1.3	0.637–1.000	0.218	0.045	0.704
	Total	*149*	*282.6–333.1*	*0.2–1.4*	*0.592–1.000*	*0.291*	*−0.031*	*1.425*

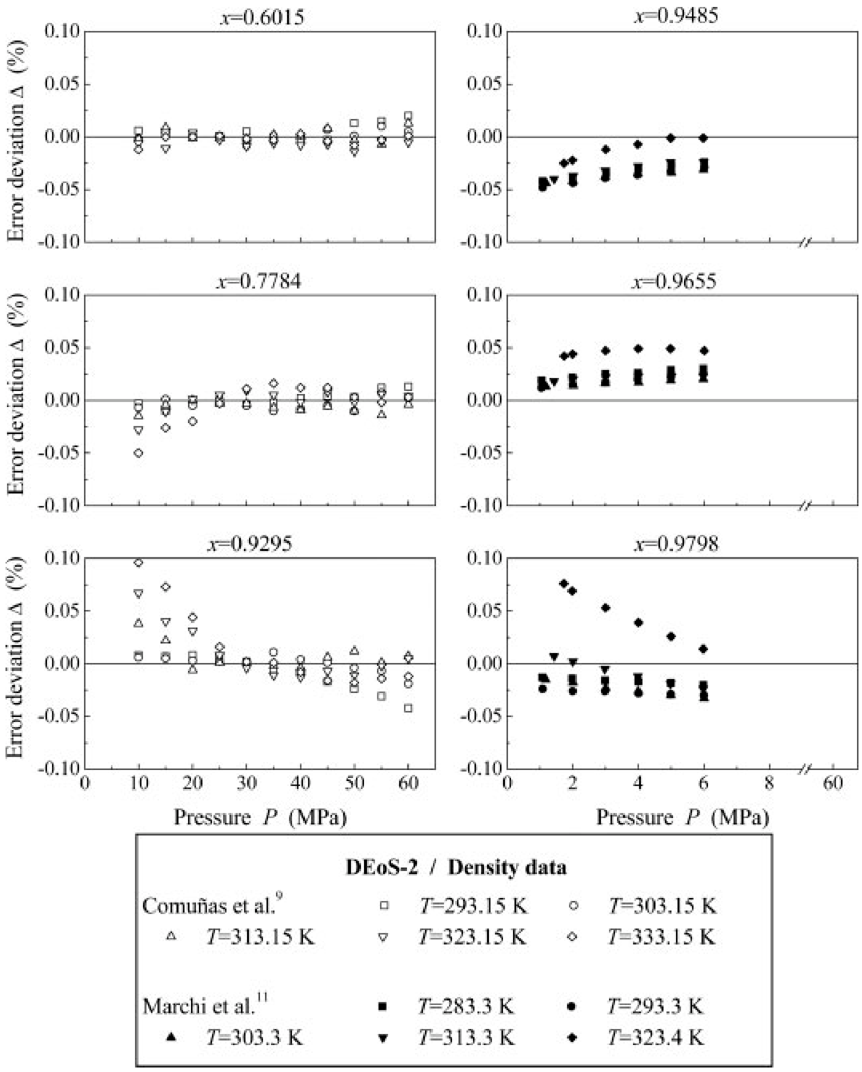

Figure 5. Deviations of the available experimental density data from DEoS-2.

($\bar{w}_{ij}$ and $\bar{w}_{ik}$) was done using a limited number of data that were measured specifically for this work.[7,11] The chosen range is representative of the refrigeration plants operating conditions.

An equation with a wider validity range was obtained by including other data available in the literature for the same system.[4,9] In this second case, the chosen number of neurons in the hidden layer is five ($J = 5$), implying 32 parameters to be determined.

The parameters of the equations, respectively indicated with DEoS-1 and DEoS-2, are reported in Tables 2 and 3, while their validity ranges are given in Table 4. Even if the equations can be slightly extrapolated outside their validity limits without significant decrease of accuracy, in particular for pressure, we strongly recommend that extrapolations are not made beyond the limits reported in Tables 2 and 3.

Validation

The performances of the equations with respect to the experimental data were evaluated in terms of relative deviation (Δ), average absolute deviation (AAD), bias (Bias), and maximum absolute deviation (MAD). Such indexes are defined as:

$$\Delta_i = \left(\frac{m_{\mathrm{exp}} - m_{\mathrm{calc}}}{m_{\mathrm{exp}}} \right)_i \tag{25}$$

$$\mathrm{AAD}\ (\%) = \frac{100}{\mathrm{NPT}} \sum_{i=1}^{\mathrm{NPT}} \left| \Delta_i \right| \tag{26}$$

$$\mathrm{Bias}\ (\%) = \frac{100}{\mathrm{NPT}} \sum_{i=1}^{\mathrm{NPT}} \Delta_i \tag{27}$$

$$\mathrm{MAD}\ (\%) = \underset{i=1,\mathrm{NPT}}{\mathrm{Max}} \left| \Delta_i \right| \tag{28}$$

where m indicates a generic thermodynamic property, NPT is the number of experimental points, and the subscripts exp and calc stand for experimental and calculated values, respectively.

The overall deviations from the experimental data for the equation valid in the narrower validity range, DEoS-1, are reported in Table 5. Unfortunately, only the data sets used for the regression procedure are available in this range and the equation cannot then be validated with respect to independent experimental sources.

For density, the deviations of all the points are plotted in Figure 2, divided into the three considered mole fractions. The AAD value for these data is 0.017%, with a maximum error of 0.054%; such values are very low and have a magnitude close to the experimental uncertainty of the present density measurements. The bias is very close to zero and this indicates that the equation is centered with respect to the data, even if a limited shifting for some isotherms is shown in Figure 2.

Bubble pressure as a function of liquid mole fraction along some isotherms is shown in Figure 3. The lines were calculated from DEoS-1; the experimental points from Marchi et al.[7] are also reported. The representation of the experimental data is very good, as is confirmed by the 0.15% AAD and by the other statistical data given in Table 5, showing also that this property is reproduced within the experimental error of the data.

DEoS-1 was then used to generate values of density, isobaric heat capacity, and speed of sound as functions of temperature at fixed mole fraction and for two selected values of pressure; the obtained lines are plotted in Figure 4. Although isobaric heat capacity and speed of sound data were not included into the regression, their predicted trends are reasonable and correspond to the expected behavior. Unfortunately, no experimental data for these properties are available for the present mixture and consequently the performances of DEoS-1 cannot be quantitatively evaluated with respect to these two quantities. However, the results obtained in a previous work[24] show that the representation of such properties can be generally considered as reliable.

A similar validation was also done for the DEoS-2 equation dedicated to a wider composition range. The overall deviations from the experimental data used in the regression are given in Table 6.

The density is represented with very low AAD values for both experimental data sets, even if the plots in Figure 5 show that the data of Marchi et al.[11] are affected by a slight systematic composition-dependent deviation.

The graph in Figure 6 for bubble pressure proves that DEoS-2 can reproduce this property with high accuracy over the whole composition range that is considered here. Anyway, Table 6 shows a limited inconsistency between the data of Marchi et al.[7] and the data of Coronas et al.[4] In fact, the second data set has a high bias value and appears as shifted with respect to the first one.

Values of density, isobaric heat capacity, and speed of sound as functions of temperature at fixed mole fraction and pressure, as previously calculated with DEoS-1, have also been calculated with DEoS-2; the results are shown in Figure 7. The lack of experimental data, apart from density, prevents from verifying whether the generated values agree with the real behavior of the mixture. The anomalous trends of some isobaric heat capacity lines at 50 MPa, see Figure 7, indicate that there are probably some deficiencies. In the present case, where the distribution of the experimental data is not homogeneous, it would have been preferable to fit the equation using also some isobaric heat capacity and speed of sound data to improve their representation. Unfortunately, data for these quantities are not available in the literature.

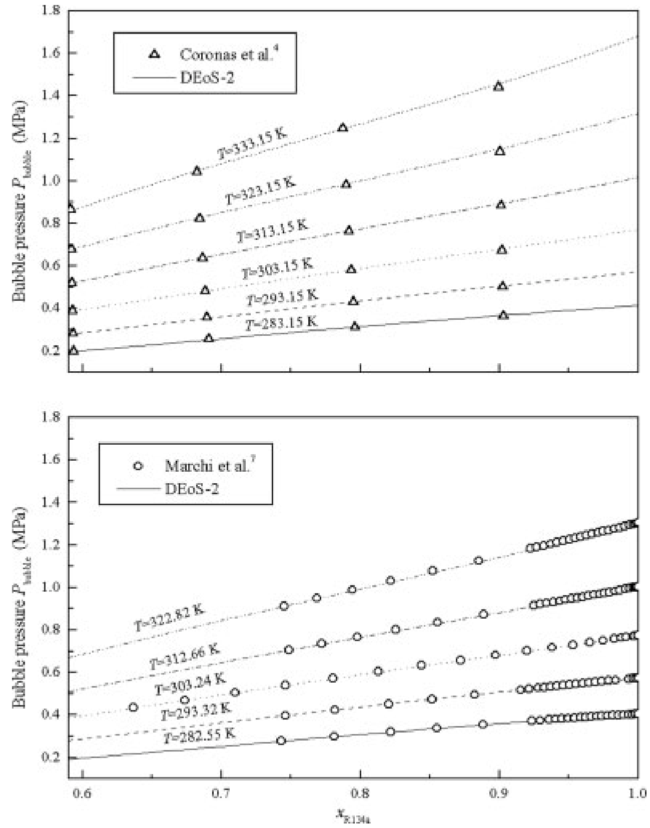

Figure 6. Bubble pressure as a function of liquid mole fraction, obtained from DEoS-2 and experimental data.

Conclusions

In this work, a mixture representative of a refrigerant + lubricant system was considered. R134a is a widely used fluid belonging to new generation of the haloalkane refrigerants, while TriEGDME is a pure compound that can be regarded as representative of a technical lubricant based on polyalkylene glycols.

Similar systems are very interesting for refrigeration and air-conditioning applications, because the substitution of the chlorofluorocarbon refrigerants with the new-generation ones has posed the problem of both the selection of suitable lubricants and the thermodynamic characterization of the refrigerant + lubricant mixtures.

A modeling approach based on the extended corresponding states technique integrated with a function approximator in the form of a neural network was adopted here. The present equation of state for mixtures, expressed in terms of Helmholtz energy, is a fundamental equation from which any thermodynamic property can be calculated through mathematical derivations.

A great advantage of this technique is that the thermodynamic representation of the lubricant, that can be either a pure

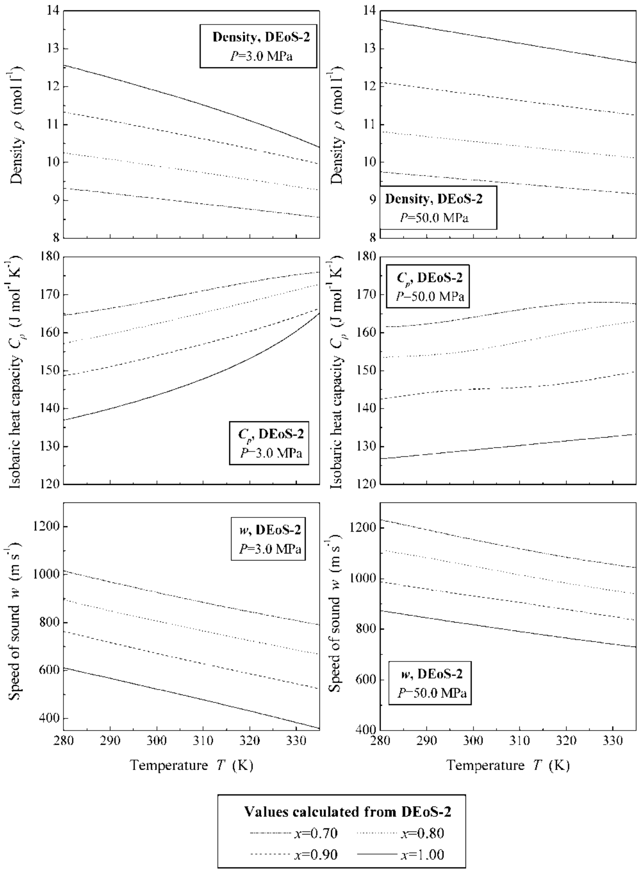

Figure 7. Values of density, isobaric heat capacity, and speed of sound at fixed mole fraction and pressure, generated from DEoS-2.

compound as in this case or a mixture as in the case of a technical lubricant, is not required. In fact, after the development of a very accurate DEoS for the refrigerant + lubricant mixture, the lubricant can be still left thermodynamically unknown.

Two equations of state were developed, basing them on the available experimental data for the chosen system. The first one was obtained from data specifically measured for this modeling work and it covers the composition range that is usual for a refrigeration plant. The second equation was regressed from a larger data base, including also other available literature data, and it has a wider validity range.

For both equations, the representation of density and bubble pressure is excellent; the experimental data are reproduced within their experimental uncertainties. The trends of the other thermodynamic properties are reasonable, but they cannot be quantitatively checked because of the lack of suitable experimental data.

The obtained results show the potentiality and the accuracy of the proposed modeling technique. The application of this method can be effectively extended to asymmetric systems similar to the present one, but not necessarily related to the refrigeration field, even where one of the components is practically unknown from the thermodynamic point of view.

Acknowledgments

One of the authors (P.M.) thanks Deutscher Akademischer Austausch Dienst (Germany) and Fondazione Gini (Italy) for the financial support.

Literature Cited

1. Marsh KN, Kandil ME. Review of thermodynamic properties of refrigerants + lubricant oils. *Fluid Phase Equilib.* 2002;199:319–334.
2. Tseregounis SI, Riley MJ. Solubility of HFC-134a refrigerant in glycol type compounds: effects of glycol structure. *AIChE J.* 1994;40:726–737.
3. Borde I, Jelinek M, Daltrophe NC. Absorption system based on the refrigerant R134a. *Int J Refrig.* 1995;18:387–394.
4. Coronas A, Mainar AM, Patil KR, Conesa A, Shen S, Zhu S. Solubility of 1,1,1,2-tetrafluoroethane in triethylene glycol dimethyl ether. *J Chem Eng Data.* 2002;47:56–58.
5. Park YM, Kang JO, Yoo J, Lee JW. Vapor pressure of the 1,1,1,2-tetrafluoroethane (R-134a) + polyalkylene glycol system. *Int J Thermophys.* 2004;25:1849–1861.
6. López ER, Mainar AN, García J, Urieta JS, Fernández J. Experimental and predicted solubilities of HFC134a (1,1,1,2-tetrafluoroethane) in polyethers. *Ind Eng Chem Res.* 2004;43:1523–1529.
7. Marchi P, Scalabrin G, Ihmels EC, Fischer K, Gmehling J. Bubble pressure measurements for the (1,1,1,2-tetrafluoroethane + triethylene glycol dimethyl ether) system. *J Chem Thermodyn.* 2006;38:1247–1253.
8. Kumagai A, Mochida H, Takahashi S. Liquid viscosities and densities of HFC-134a + glycol mixtures. *Int J Thermophys.* 1993;14:45–53.
9. Comuñas MJP, Fernández J, Baylaucq A, Canet X, Boned C. PρTx measurements for HFC-134a + triethylene glycol dimethylether system. *Fluid Phase Equilib.* 2002;199:185–195.
10. Comuñas MJP, Baylaucq A, Boned C, Canet X, Fernández J. High-pressure volumetric behavior of x 1,1,1,2-tetrafluoroethane + (1 −x) 2,5,8,11,14-pentaoxapentadecane (TEGDME) mixtures. *J Chem Eng Data.* 2002;47:233–238.
11. Marchi P, Scalabrin G, Ihmels EC, Fischer K, Gmehling J. $P\rho Tx$ measurements for (1,1,1,2-tetrafluoroethane + triethylene glycol dimethylether) at high haloalkane content. *J Chem Eng Data.* 2006;51:992–996.
12. Kumagai A, Miura-Mochida H, Takahashi S. Revised viscosities for HFC-134a + glycol mixtures from 273 to 333 K. *Int J Thermophys.* 1994;15:109–115.
13. Comuñas MJP, Baylaucq A, Boned C, Fernández J. Dynamic viscosity for HFC-134a + polyether mixtures up to 373.15 K and 140 MPa at low polyether concentration. Measurements and modeling. *Ind Eng Chem Res.* 2004;43:804–814.
14. Monsalvo MA, Baylaucq A, Reghem P, Quiñones-Cisneros SE, Boned C. Viscosity measurements and correlations of binary mixtures: 1,1,1,2-tetrafluoroethane (HFC-134a) + tetraethylene glycol dimethylether (TEGDME). *Fluid Phase Equilib.* 2005;233:1–8.
15. Martz WL, Burton CM, Jacobi AM. Local composition modelling of the thermodynamic properties of refrigerant and oil mixtures. *Int J Refrig.* 1996;19:25–33.
16. Bertucco A, Elvassore N, Fermeglia M, Prausnitz JM. A perturbed-hard-sphere-chain equation of state for phase equilibria of mixtures containing a refrigerant and a lubricant oil. *Fluid Phase Equilib.* 1999;158–160:183–191.
17. Elvassore N, Bertucco A, Wahlström Å. A cubic equation of state with group contributions for the calculation of vapor-liquid equilibria of mixtures of hydrofluorocarbons and lubricant oils. *Ind Eng Chem Res.* 1999;38:2110–2118.
18. Huber ML, Holcomb CD, Outcalt SL, Elliott JR. Vapor-liquid equilibria for a lubricant mixture: measurements and equation-of-state modeling. *ASHRAE Trans.* 2000;106:768–773.
19. Huber ML, Lemmon EW, Friend DG. Modeling bubble points of mixtures of hydrofluorocarbon refrigerants and polyol ester lubricants. *Fluid Phase Equilib.* 2002;194:511–519.
20. Wahlström Å, Vamling L. Development of models for prediction of solubility for HFC working fluids in pentaerythritol ester compressor oils. *Int J Refrig.* 2000;23:597–608.

21. Yokozeki A. Solubility of refrigerants in various lubricants. *Int J Thermophys*. 2001;22:1057–1071.
22. Teodorescu M, Lugo L, Fernández J. Modeling of gas solubility data for HFCs-lubricant oil binary systems by means of the SRK equation of state. *Int J Thermophys*. 2003;24:1043–1060.
23. Scalabrin G, Piazza L, Richon D. An equation of state for R227ea from density data through a new extended corresponding states-neural network technique. *Fluid Phase Equilib*. 2002;199: 33–51.
24. Scalabrin G, Marchi P, Bettio L, Richon D. Enhancement of the extended corresponding states techniques for thermodynamic modeling. II. Mixtures. *Int J Refrig*. 2006;29:1195–1207.
25. Piazza L, Scalabrin G, Marchi P, Richon D. Enhancement of the extended corresponding states techniques for thermodynamic modeling. I. Pure fluids. *Int J Refrig*. 2006;29:1182–1194.
26. Reed TM, Gubbins KE. *Applied Statistical Mechanics*. New York: McGraw-Hill, 1973.
27. Rowlinson JS, Swinton FL. *Liquids and Liquid Mixtures*. Oxford: Butterworth, 1982.
28. Leland TW, Chappelear PS. The corresponding states principle. A review of current theory and practice. *Ind Eng Chem*. 1968;60: 15–43.
29. Rowlinson JS, Watson ID. The prediction of the thermodynamic properties of fluid and fluid mixtures. I. The principle of corresponding states and its extensions. *Chem Eng Sci*. 1969;24:1565–1574.
30. Fisher GD, Leland TW. Corresponding states principle using shape factors. *Ind Eng Chem Fundam*. 1970;9:537–544.
31. Ely JF. A predictive, exact shape factor extended corresponding states model for mixtures. *Adv Cryog Eng*. 1990;35:1511–1520.
32. Huber ML, Ely JF. A predictive extended corresponding states model for pure and mixed refrigerants including an equation of state for R134a. *Int J Refrig*. 1994;17:18–31.
33. Ely JF, Marrucho IMF. The corresponding-states principle. In: Sengers JV, Kayser RF, Peters CJ, White HJ Jr editors. *Equations of State for Fluids and Fluid Mixtures*. I. Amsterdam: Elsevier, 2000: 289–320.
34. Estela-Uribe JF, Trusler JPM. Shape factors for the light hydrocarbons. *Fluid Phase Equilib*. 1998;150/151:225–234.
35. Estela-Uribe JF, Trusler JPM. Extended corresponding states equation of state for natural gas systems. *Fluid Phase Equilib*. 2001;183/184:21–29.
36. Estela-Uribe JF, Trusler JPM. Extended corresponding states model for fluids and fluid mixtures. I. Shape factor model for pure fluids. *Fluid Phase Equilib*. 2003;204:15–40.
37. Estela-Uribe JF, Trusler JPM. Extended corresponding states model for fluids and fluid mixtures. II. Application to mixtures and natural gas systems. *Fluid Phase Equilib*. 2003;216:59–84.
38. Astina IM, Sato H. A fundamental equation of state for 1,1,1,2-tetrafluoroethane with an intermolecular potential energy background and reliable ideal-gas properties. *Fluid Phase Equilib*. 2004;221:103–111.
39. Poling BE, Prausnitz JM, O'Connell JP. *The Properties of Gases and Liquids*, 5th ed. New York: McGraw-Hill, 2001.
40. Mohr PJ, Taylor BN. CODATA recommended values of the fundamental physical constants: 1998. *Rev Mod Phys*. 2000;72:351–495.

Appendix A: Thermodynamic Properties from a Helmholtz Energy Equation of State

The availability of a Helmholtz energy equation for the system allows the calculation of all its thermodynamic properties simply through mathematical derivations. The relations between Helmholtz energy and other properties are given here.

Table A1. Calculation of Thermodynamic Properties

Property	Relation	Equation no.
Compressibility factor	$Z \equiv P/\rho RT = 1 + \rho a_\rho^{\mathrm{R}}$	A8
Internal energy	$U/RT = -T\left(a_T^{\mathrm{ig}} + a_T^{\mathrm{R}}\right)$	A9
Enthalpy	$H/RT = 1 - T\left(a_T^{\mathrm{ig}} + a_T^{\mathrm{R}}\right) + \rho a_\rho^{\mathrm{R}}$	A10
Gibbs energy	$G/RT = 1 + a^{\mathrm{ig}} + a^{\mathrm{R}} + \rho a_\rho^{\mathrm{R}}$	A11
Helmholtz energy	$A/RT = a^{\mathrm{ig}} + a^{\mathrm{R}}$	A12
Entropy	$S/R = -T\left(a_T^{\mathrm{ig}} + a_T^{\mathrm{R}}\right) - a^{\mathrm{ig}} - a^{\mathrm{R}}$	A13
Isochoric heat capacity	$C_v/R = -T^2\left(a_{TT}^{\mathrm{ig}} + a_{TT}^{\mathrm{R}}\right) - 2T\left(a_T^{\mathrm{ig}} + a_T^{\mathrm{R}}\right)$	A14
Isobaric heat capacity	$C_p/R = C_v/R + \dfrac{\left(1 + \rho a_\rho^{\mathrm{R}} + \rho T a_{\rho T}^{\mathrm{R}}\right)^2}{1 + 2\rho a_\rho^R + \rho^2 a_{\rho\rho}^R}$	A15
Speed of sound	$w^2 M/RT = \left(1 + 2\rho a_\rho^{\mathrm{R}} + \rho^2 a_{\rho\rho}^{\mathrm{R}}\right) C_p/C_v$	A16
Fugacity coefficient	$\ln \varphi = Z - 1 - \ln Z + a^{\mathrm{R}}$	A17
Partial molar fugacity coefficient of component i in mixture*	$\ln \hat{\varphi}_i = a^{\mathrm{R}} - \ln Z + n\left(\partial a^{\mathrm{R}}/\partial n_i\right)_{T,V_{\mathrm{TOT}},n_{j\neq i}}$	A18
Fugacity of component i in mixture	$\hat{f}_i = x_i \hat{\varphi}_i P$	A19
Joule-Thomson coefficient	$\mu_J = (\partial T/\partial P)_H = (T\beta - 1)/\rho C_p$	A20

*The total number of moles is denoted with n, while the number of moles of component i is indicated with n_i; V_{TOT} is the total volume of the mixture.

Definitions

$$a_T^{\mathrm{ig}} \equiv \left(\frac{\partial a^{\mathrm{ig}}}{\partial T}\right)_{\rho,\bar{x}} \qquad a_{TT}^{\mathrm{ig}} \equiv \left(\frac{\partial^2 a^{\mathrm{ig}}}{\partial T^2}\right)_{\rho,\bar{x}} \qquad a_\rho^{\mathrm{R}} \equiv \left(\frac{\partial a^{\mathrm{R}}}{\partial \rho}\right)_{T,\bar{x}}$$

$$a_T^{\mathrm{R}} \equiv \left(\frac{\partial a^{\mathrm{R}}}{\partial T}\right)_{\rho,\bar{x}} \qquad \text{(A1, A2, A3, A4)}$$

$$a_{\rho\rho}^{\mathrm{R}} \equiv \left(\frac{\partial^2 a^{\mathrm{R}}}{\partial \rho^2}\right)_{T,\bar{x}} \qquad a_{TT}^{\mathrm{R}} \equiv \left(\frac{\partial^2 a^{\mathrm{R}}}{\partial T^2}\right)_{\rho,\bar{x}} \qquad a_{\rho T}^{\mathrm{R}} \equiv \left(\frac{\partial^2 a^{\mathrm{R}}}{\partial \rho\, \partial T}\right) \qquad \text{(A5, A6, A7)}$$

Appendix B: Helmholtz Energy Derivatives in the ECS Format

The analytical expressions of the derivatives of the Helmholtz energy for a mixture equation of state in the ECS format are given here. The thermodynamic properties of the mixture are calculated by substituting these derivatives into the equations in Appendix A.

Definitions of the logarithmical derivatives of the scale factors

$$F_\rho \equiv \frac{\rho_{\mathrm{m}}}{f_{\mathrm{m}}}\left(\frac{\partial f_{\mathrm{m}}}{\partial \rho_{\mathrm{m}}}\right)_{T_{\mathrm{m}},\bar{x}} \qquad H_\rho \equiv \frac{\rho_{\mathrm{m}}}{h_{\mathrm{m}}}\left(\frac{\partial h_{\mathrm{m}}}{\partial \rho_{\mathrm{m}}}\right)_{T_{\mathrm{m}},\bar{x}} \qquad \text{(B1, B2)}$$

$$F_T \equiv \frac{T_{\mathrm{m}}}{f_{\mathrm{m}}}\left(\frac{\partial f_{\mathrm{m}}}{\partial T_{\mathrm{m}}}\right)_{\rho_{\mathrm{m}},\bar{x}} \qquad H_T \equiv \frac{T_{\mathrm{m}}}{h_{\mathrm{m}}}\left(\frac{\partial h_{\mathrm{m}}}{\partial T_{\mathrm{m}}}\right)_{\rho_{\mathrm{m}},\bar{x}} \qquad \text{(B3, B4)}$$

$$F_{\rho\rho} \equiv \frac{\rho_{\mathrm{m}}^2}{f_{\mathrm{m}}}\left(\frac{\partial^2 f_{\mathrm{m}}}{\partial \rho_{\mathrm{m}}^2}\right)_{T_{\mathrm{m}},\bar{x}} \qquad H_{\rho\rho} \equiv \frac{\rho_{\mathrm{m}}^2}{h_{\mathrm{m}}}\left(\frac{\partial^2 h_{\mathrm{m}}}{\partial \rho_{\mathrm{m}}^2}\right)_{T_{\mathrm{m}},\bar{x}} \qquad \text{(B5, B6)}$$

$$F_{TT} \equiv \frac{T_{\mathrm{m}}^2}{f_{\mathrm{m}}}\left(\frac{\partial^2 f_{\mathrm{m}}}{\partial T_{\mathrm{m}}^2}\right)_{\rho_{\mathrm{m}},\bar{x}} \qquad H_{TT} \equiv \frac{T_{\mathrm{m}}^2}{h_{\mathrm{m}}}\left(\frac{\partial^2 h_{\mathrm{m}}}{\partial T_{\mathrm{m}}^2}\right)_{\rho_{\mathrm{m}},\bar{x}} \qquad \text{(B7, B8)}$$

$$F_{\rho T} \equiv \frac{\rho_{\mathrm{m}} T_{\mathrm{m}}}{f_{\mathrm{m}}}\left(\frac{\partial^2 f_{\mathrm{m}}}{\partial \rho_{\mathrm{m}} \partial T_{\mathrm{m}}}\right)_{\bar{x}} \qquad H_{\rho T} \equiv \frac{\rho_{\mathrm{m}} T_{\mathrm{m}}}{h_{\mathrm{m}}}\left(\frac{\partial^2 h_{\mathrm{m}}}{\partial \rho_{\mathrm{m}} \partial T_{\mathrm{m}}}\right)_{\bar{x}} \qquad \text{(B9, B10)}$$

$$F_{n_i} = \frac{n}{f_{\mathrm{m}}}\left(\frac{\partial f_{\mathrm{m}}}{\partial n_i}\right)_{T_{\mathrm{m}},\rho_{\mathrm{m}},n_{j\neq i}} = \frac{1}{f_{\mathrm{m}}}\left\{\left(\frac{\partial f_{\mathrm{m}}}{\partial x_i}\right)_{T_{\mathrm{m}},\rho_{\mathrm{m}},x_{j\neq i}} - \sum_{k=1}^{N_{\mathrm{comp}}}\left[x_k\left(\frac{\partial f_{\mathrm{m}}}{\partial x_k}\right)_{T_{\mathrm{m}},\rho_{\mathrm{m}},x_{j\neq k}}\right]\right\} \qquad \text{(B11)}$$

$$H_{n_i} = \frac{n}{h_{\mathrm{m}}}\left(\frac{\partial h_{\mathrm{m}}}{\partial n_i}\right)_{T_{\mathrm{m}},\rho_{\mathrm{m}},n_{j\neq i}} = \frac{1}{h_{\mathrm{m}}}\left\{\left(\frac{\partial h_{\mathrm{m}}}{\partial x_i}\right)_{T_{\mathrm{m}},\rho_{\mathrm{m}},x_{j\neq i}} - \sum_{k=1}^{N_{\mathrm{comp}}}\left[x_k\left(\frac{\partial h_{\mathrm{m}}}{\partial x_k}\right)_{T_{\mathrm{m}},\rho_{\mathrm{m}},x_{j\neq k}}\right]\right\} \qquad \text{(B12)}$$

In the present case of a binary mixture, Eqs. B11 and B12 for R134a can be rewritten in the following forms, where x is the molar fraction of refrigerant:

$$F_{n_1} = \frac{(1-x)}{f_{\mathrm{m}}}\left(\frac{\partial f_{\mathrm{m}}}{\partial x}\right)_{T_{\mathrm{m}},\rho_{\mathrm{m}}} H_{n_1} = \frac{(1-x)}{h_{\mathrm{m}}}\left(\frac{\partial h_{\mathrm{m}}}{\partial x}\right)_{T_{\mathrm{m}},\rho_{\mathrm{m}}} \qquad \text{(B13, B14)}$$

Derivatives of the Helmholtz energy

As explained in The Equations of State for the (R134a + TriEGDME) System section, the subscript m denotes mixture properties at (T_{m}, ρ_{m}, $\bar{x}$) conditions; the subscript 0 denotes the properties of the reference fluid, calculated from its equation of state at (T_0, ρ_0).

$$T_0 = T_{\mathrm{m}}/f_{\mathrm{m}} \qquad \rho_0 = \rho_{\mathrm{m}} h_{\mathrm{m}} \qquad \text{(B15, B16)}$$

$$\rho_{\mathrm{m}} a_{\mathrm{m},\rho}^{\mathrm{R}} \equiv \rho_{\mathrm{m}}\left(\frac{\partial a_{\mathrm{m}}^{\mathrm{R}}}{\partial \rho_{\mathrm{m}}}\right)_{T_{\mathrm{m}},\bar{x}} = \rho_0 a_{0,\rho}^{\mathrm{R}}\left(1+H_\rho\right) - T_0 a_{0,T}^{\mathrm{R}} F_\rho \qquad \text{(B17)}$$

$$T_{\mathrm{m}} a_{\mathrm{m,T}}^{\mathrm{R}} \equiv T_{\mathrm{m}}\left(\frac{\partial a_{\mathrm{m}}^{\mathrm{R}}}{\partial T_{\mathrm{m}}}\right)_{\rho_{\mathrm{m}},\bar{x}} = \rho_0 a_{0,\rho}^{\mathrm{R}} H_T + T_0 a_{0,T}^{\mathrm{R}}\left(1-F_T\right) \qquad \text{(B18)}$$

$$\begin{aligned}\rho_{\mathrm{m}}^2 a_{\mathrm{m},\rho\rho}^{\mathrm{R}} \equiv \rho_{\mathrm{m}}^2\left(\frac{\partial^2 a_{\mathrm{m}}^{\mathrm{R}}}{\partial \rho_{\mathrm{m}}^2}\right)_{T_{\mathrm{m}},\bar{x}} &= \rho_0^2 a_{0,\rho\rho}^{\mathrm{R}}\left(1+H_\rho\right)^2 \\ &+ \rho_0 a_{0,\rho}^{\mathrm{R}}\left(2H_\rho + H_{\rho\rho}\right) + -2\rho_0 T_0 a_{0,\rho T}^{\mathrm{R}} F_\rho\left(1+H_\rho\right) \\ &+ T_0 a_{0,T}^{\mathrm{R}}\left(2F_\rho^2 - F_{\rho\rho}\right) + T_0^2 a_{0,TT}^{\mathrm{R}} F_\rho^2 \end{aligned} \qquad \text{(B19)}$$

$$\begin{aligned}T_{\mathrm{m}}^2 a_{\mathrm{m},TT}^{\mathrm{R}} \equiv T_{\mathrm{m}}^2\left(\frac{\partial^2 a_{\mathrm{m}}^{\mathrm{R}}}{\partial T_{\mathrm{m}}^2}\right)_{\rho_{\mathrm{m}},\bar{x}} &= \rho_0^2 a_{0,\rho\rho}^{\mathrm{R}} H_T^2 + \rho_0 a_{0,\rho}^{\mathrm{R}} H_{TT} \\ &+ 2\rho_0 T_0 a_{0,\rho T}^{\mathrm{R}} H_T\left(1-F_T\right) + T_0 a_{0,T}^{\mathrm{R}}\left(2F_T^2 - 2F_T - F_{TT}\right) \\ &+ T_0^2 a_{0,TT}^{\mathrm{R}}\left(1-F_T\right)^2 \end{aligned} \qquad \text{(B20)}$$

$$\begin{aligned}\rho_{\mathrm{m}} T_{\mathrm{m}} a_{\mathrm{m},\rho T}^{\mathrm{R}} \equiv \rho_{\mathrm{m}} T_{\mathrm{m}}\left(\frac{\partial^2 a_{\mathrm{m}}^{\mathrm{R}}}{\partial \rho_{\mathrm{m}} \partial T_{\mathrm{m}}}\right) &= \rho_0^2 a_{0,\rho\rho}^{\mathrm{R}} H_T\left(1+H\rho\right) \\ &+ \rho_0 a_{0,\rho}^{\mathrm{R}}\left(H_T + H_{\rho T}\right) + \rho_0 T_0 a_{0,\rho T}^{\mathrm{R}}\left[\left(1+H_\rho\right)\left(1-F_T\right) - F_\rho H_T\right] \\ &+ T_0 a_{0,T}^{\mathrm{R}}\left(2F_T F_\rho - F_\rho - F_{\rho T}\right) + T_0^2 a_{0,TT}^{\mathrm{R}} F_\rho\left(F_T - 1\right) \end{aligned} \qquad \text{(B21)}$$

$$\ln\hat{\varphi}_i = \ln\varphi_0 - \ln\left(Z_{\mathrm{m}}/Z_0\right) - T_0 a_{0,T}^{\mathrm{R}}\left(F_{n_i} + F_\rho\right) + \rho_0 a_{0,\rho}^{\mathrm{R}}\left(H_{n_i} + H_\rho\right) \qquad \text{(B22)}$$

Appendix C: Derivatives of the Scale Factors in Neural Network Form

In the present work, the scale factors are obtained in the form of a multilayer feedforward neural network. The expressions for the calculation of the scale factors and their derivatives are reported in the following. The correspondence of the physical variables with the variables of the neural model is given by:

$$V_1 = T_{\mathrm{m}} \qquad V_2 = \rho_{\mathrm{m}} \qquad V_3 = x \qquad \text{(C1, C2, C3)}$$

$$W_1 = \widetilde{f}_{\mathrm{m}} \quad W_2 = \widetilde{h}_{\mathrm{m}} \qquad \text{(C4, C5)}$$

Neural network inputs

$$U_i = u_i\left(V_i - V_{i,\min}\right) + A_{\min} \quad 1 \le i \le I-1 \tag{C6}$$

$$U_I = \text{Bias 1} \tag{C7}$$

with

$$u_i = \frac{A_{\max} - A_{\min}}{V_{i,\max} - V_{i,\min}} \tag{C8}$$

Hidden layer inputs and outputs

$$G_j = \sum_{i=1}^{I} w_{ij} U_i \quad 1 \le j \le J \tag{C9}$$

$$H_j = g(G_j) \quad 1 \le j \le J \tag{C10}$$

$$H_{J+1} = \text{Bias2} \tag{C11}$$

Output layer inputs and outputs

$$R_k = \sum_{j=1}^{J+1} w_{jk} H_j \quad 1 \le k \le K \tag{C12}$$

$$S_k = g(R_k) \quad 1 \le k \le K \tag{C13}$$

Physical variable outputs

$$W_k = \frac{S_k - A_{\min}}{s_k} + W_{k,\min} \quad 1 \le k \le K \tag{C14}$$

with

$$s_k = \frac{A_{\max} - A_{\min}}{W_{k,\max} - W_{k,\min}} \tag{C15}$$

Output derivatives

$$\frac{\partial W_k}{\partial V_m} = \frac{u_m}{s_k} g'(R_k) \sum_{j=1}^{J} w_{mj} w_{jk} g'(G_j) \qquad 1 \le m \le I-1, 1 \le k \le K \tag{C16}$$

$$\frac{\partial^2 W_k}{\partial V_m \partial V_n} = \frac{u_m u_n}{s_k} g''(R_k) \left[\sum_{j=1}^{J} w_{mj} w_{jk} g'(G_j)\right]\left[\sum_{j=1}^{J} w_{nj} w_{jk} g'(G_j)\right] + g'(R_k)\left[\sum_{j=1}^{J} w_{mj} w_{nj} w_{jk} g''(G_j)\right] \quad 1 \le m, n \le I-1, 1 \le k \le K \tag{C17}$$

where

$$g(z) = \frac{1}{\pi} \arctan(0.1\, z) + 0.5 \tag{C18}$$

$$g'(z) = \frac{dg(z)}{dz} = \frac{0.1}{\pi\left[1 + (0.1\, z)^2\right]} \tag{C19}$$

$$g''(z) = \frac{d^2 g(z)}{dz^2} = -\frac{0.002\, z}{\pi\left[1 + (0.1\, z)^2\right]^2} \tag{C20}$$

Scale factors and their derivatives

$$f_{\mathrm{m}} = 1 + (1-x)\tilde{f}_{\mathrm{m}} \quad h_{\mathrm{m}} = 1 + (1-x)\tilde{h}_{\mathrm{m}} \tag{C21, C22}$$

$$\left(\frac{\partial f_{\mathrm{m}}}{\partial T_{\mathrm{m}}}\right)_{\rho_{\mathrm{m}},x} = \left(\frac{\partial \tilde{f}_{\mathrm{m}}}{\partial T_{\mathrm{m}}}\right)_{\rho_{\mathrm{m}},x} \quad \left(\frac{\partial h_{\mathrm{m}}}{\partial T_{\mathrm{m}}}\right)_{\rho_{\mathrm{m}},x} = \left(\frac{\partial \tilde{h}_{\mathrm{m}}}{\partial T_{\mathrm{m}}}\right)_{\rho_{\mathrm{m}},x} \tag{C23, C24}$$

$$\left(\frac{\partial f_{\mathrm{m}}}{\partial \rho_{\mathrm{m}}}\right)_{T_{\mathrm{m}},x} = \left(\frac{\partial \tilde{f}_{\mathrm{m}}}{\partial \rho_{\mathrm{m}}}\right)_{T_{\mathrm{m}},x} \quad \left(\frac{\partial h_{\mathrm{m}}}{\partial \rho_{\mathrm{m}}}\right)_{T_{\mathrm{m}},x} = \left(\frac{\partial \tilde{h}_{\mathrm{m}}}{\partial \rho_{\mathrm{m}}}\right)_{T_{\mathrm{m}},x} \tag{C25, C26}$$

$$\left(\frac{\partial^2 f_{\mathrm{m}}}{\partial T_{\mathrm{m}}^2}\right)_{\rho_{\mathrm{m}},x} = \left(\frac{\partial^2 \tilde{f}_{\mathrm{m}}}{\partial T_{\mathrm{m}}^2}\right)_{\rho_{\mathrm{m}},x} \quad \left(\frac{\partial^2 h_{\mathrm{m}}}{\partial T_{\mathrm{m}}^2}\right)_{\rho_{\mathrm{m}},x} = \left(\frac{\partial^2 \tilde{h}_{\mathrm{m}}}{\partial T_{\mathrm{m}}^2}\right)_{\rho_{\mathrm{m}},x} \tag{C27, C28}$$

$$\left(\frac{\partial^2 f_{\mathrm{m}}}{\partial \rho_{\mathrm{m}}^2}\right)_{T_{\mathrm{m}},x} = \left(\frac{\partial^2 \tilde{f}_{\mathrm{m}}}{\partial \rho_{\mathrm{m}}^2}\right)_{T_{\mathrm{m}},x} \quad \left(\frac{\partial^2 h_{\mathrm{m}}}{\partial \rho_{\mathrm{m}}^2}\right)_{T_{\mathrm{m}},x} = \left(\frac{\partial^2 \tilde{h}_{\mathrm{m}}}{\partial \rho_{\mathrm{m}}^2}\right)_{T_{\mathrm{m}},x} \tag{C29, C30}$$

$$\left(\frac{\partial^2 f_{\mathrm{m}}}{\partial \rho_{\mathrm{m}} \partial T_{\mathrm{m}}}\right)_{x} = \left(\frac{\partial^2 \tilde{f}_{\mathrm{m}}}{\partial \rho_{\mathrm{m}} \partial T_{\mathrm{m}}}\right)_{x} \quad \left(\frac{\partial^2 h_{\mathrm{m}}}{\partial \rho_{\mathrm{m}} \partial T_{\mathrm{m}}}\right)_{x} = \left(\frac{\partial^2 \tilde{h}_{\mathrm{m}}}{\partial \rho_{\mathrm{m}} \partial T_{\mathrm{m}}}\right)_{x} \tag{C31, C32}$$

$$\left(\frac{\partial f_{\mathrm{m}}}{\partial x}\right)_{T_{\mathrm{m}},\rho_{\mathrm{m}}} = -\tilde{f}_{\mathrm{m}} + (1-x)\left(\frac{\partial \tilde{f}_{\mathrm{m}}}{\partial x}\right)_{T_{\mathrm{m}},\rho_{\mathrm{m}}} \tag{C33}$$

$$\left(\frac{\partial h_{\mathrm{m}}}{\partial x}\right)_{T\mathrm{m},\rho_{\mathrm{m}}} = -\tilde{h}_{\mathrm{m}} + (1-x)\left(\frac{\partial \tilde{h}_{\mathrm{m}}}{\partial x}\right)_{T_{\mathrm{m}},\rho_{\mathrm{m}}} \tag{C34}$$

Manuscript received Aug. 27, 2006, and revision received Feb. 14, 2007.